Assessing the Impact of the Space Radiation Environment on Parametric Degradation and Single-Event Transients in Optocouplers

Robert A. Reed, *Member, IEEE*, Christian Poivey, *Member, IEEE*, Paul W. Marshall, *Member, IEEE*, Kenneth A. LaBel, *Member, IEEE*, Cheryl J. Marshall, *Member, IEEE*, Scott Kniffin, *Member, IEEE*, Janet L. Barth, *Senior Member, IEEE*, and Christina Seidleck, *Member, IEEE*

***Abstract*—Assessing the risk of using optocouplers in satellite applications offers challenges that incorporate those of commercial off-the-shelf devices compounded by hybrid module construction techniques. We discuss approaches for estimating this risk. In the process, we benchmark our estimates for proton and heavy-ion induced single-event transient rate estimates with recent flight data from the Terra mission. For parametric degradation, we discuss a method for acquiring test data and mapping it into an estimation approach that captures all the important variables of circuit application, environment, damage energy dependence, complex response to total ionizing dose and displacement effects, temperature, and annealing.**

***Index Terms*—Displacement damage, hardness assurance, optocouplers, single-event effects (SEEs), total ionizing dose.**

I. Introduction

OPTOCOUPLERS are being used increasingly both in space and in commercial systems because they provide an efficient means of electrical isolation of microelectronic circuits. As might be expected of such an increasingly popular technology, the numbers and types of these devices have proliferated. A recent check revealed that Agilent Technologies alone manufactures 55 different device types that use optocoupler technology—that is, they use light to provide electrical isolation. Optocouplers vary in design and functionality, and these differences can affect how the optocoupler responds to a radiation environment. Clearly, addressing all of the radiation effect concerns for each type of optocoupler is not feasible in this paper. Here, we will focus on radiation concerns for high-bandwidth digital signal isolators and optocouplers used to transfer current from one circuit to the next.

Fig. 1 shows a block diagram of a typical optocoupler, which includes a light-emitting diode (LED) and a photoreceiver in a single package. Typically, the receivers in high-bandwidth digital isolators are photodiodes, followed by an amplification stage. Current transfer optocouplers usually use a phototransistor or photodarlington as the receiver. See [1] and [8] for a discussion of optocoupler manufacturing techniques.

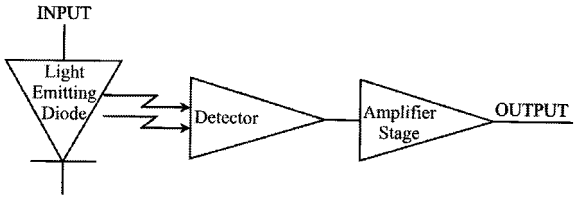

Fig. 1. Typical optocoupler design. The receiver side contains a detector and possibly a simple amplification stage [7].

Past studies have shown that optocoupler performance is adversely affected by both radiation-induced permanent damage and single-event effects [1]–[9]. Dealing with each of these effects poses its own specific challenges. At present, more research has been published on permanent damage than on single-event effects.

This paper will first consider the impact of single-event transients (SETs) and then examine issues related to permanent damage. In both sections, we describe the issues specific to each radiation effect and present new data that illustrate some of the testing concerns. In Section II, we will present an approach for predicting on-orbit performance based on ground-based test data. We will compare predicted error rates to on-orbit data for an Agilent optocoupler. In Section III, we present our current approach for assessing the impact of this type of degradation on spaceflight hardware.

Because optocouplers are hybrid devices and almost always commercial off-the-shelf (COTS) technologies, using them in spaceflight applications poses the same concerns and challenges one experiences when using other such devices. Clearly, development of a comprehensive radiation hardness assurance (RHA) plan for optocouplers will require first developing RHA plans for hybrids and COTS. Consequently, this paper does not aim at developing a rigorous RHA program for optocouplers, but rather at developing a risk analysis approach where ground testing and performance estimates can be combined with engineering judgment to understand the performance of optocouplers in spaceflight applications.

Manuscript received July 17, 2001. This work was supported by NASA Electronics Radiation Characterization Project, a portion of the NASA Electronic Parts and Packaging Program, and by the Defense Threat Reduction Agency under Contract IACRO 01-4050/0001278.

R. A. Reed, P. W. Marshall, K. A. LaBel, C. J. Marshall, and J. L. Barth are with NASA Goddard Space Flight Center, Greenbelt, MD 20771 USA.

C. Poivey is with SGT-Inc., NASA Goddard Space Flight Center, Greenbelt, MD 20771 USA.

S. Kniffin is with Orbital Sciences, NASA Goddard Space Flight Center, Greenbelt, MD 20771 USA.

C. Seidleck is with Raytheon Corporation, NASA Goddard Space Flight Center, Greenbelt, MD 20771 USA.

Publisher Item Identifier S 0018-9499(01)10712-4.

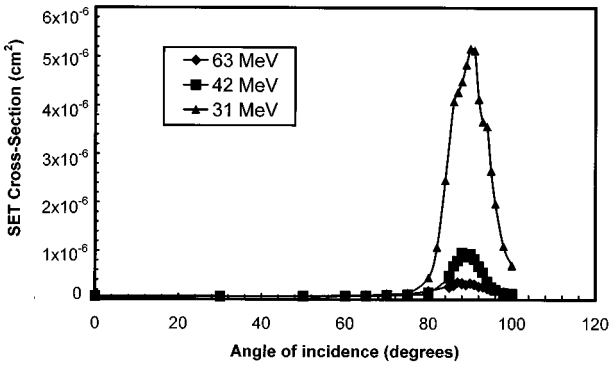

Fig. 2. Effect of incident angle on cross section of the Agilent HCPL5231 optocoupler for various proton energies.

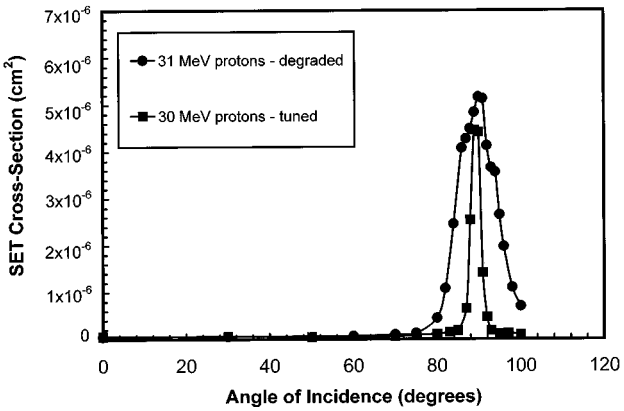

Fig. 3. Comparison of SET cross section measurement for degraded and tuned 30-MeV proton beam on the Agilent HCPL5231 optocoupler.

II. Assessment of Single-Event Transient Sensitivity

A. Introduction

Proton-induced SETs in high-speed optocouplers were reported first by LaBel *et al.* following an investigation on-board flight anomalies due to single particle event effects in optocouplers used on the Hubble Space Telescope (HST) [6].

The photodetectors used in optocouplers are very sensitive to SETs. If the transient has sufficient pulsewidth and voltage amplitude, and the optocoupler amplifier stage is of sufficient bandwidth, then an external effect may be observed at the optocoupler output. Previous test data show an unexpected increase in cross section at high angles of incidence relative to the normal [6]–[8]. These results indicated that unlike most microelectronics devices, optocouplers were susceptible to proton-induced errors from both direct ionization and indirect ionization resulting from proton–silicon interactions [6]. Not surprisingly, optocouplers that are sensitive to transient errors from protons are also sensitive to errors induced by cosmic rays. Moreover, transients generated in the high gain amplifier add to those associated with the photodetector to give the total SET cross section [14].

Fig. 2 shows an example of the increase in SET cross section with the incident angle for the Agilent HCPL5231 optocoupler for three different proton energies. At 60 MeV, the angular dependence is very weak, but for the lower energies the effect is stronger. For 42-MeV protons, the cross section at grazing incidence is a factor of ten higher than the cross section at normal incidence. For 31-MeV protons, the grazing incidence cross section increases by nearly two orders of magnitude. This dependence indicates that transients caused by direct ionization by protons traversing the diameter of the photodiode dominate at grazing incidence.

In contrast to conventional proton testing, SET characterization of optocouplers requires testing at several different angles of incidence to determine the contributions of both direct and indirect ionization by protons to optocoupler SET sensitivity.

B. Issues When Evaluating Optocoupler SETs

Below, we present a summary of the issues that should be considered when evaluating an optocoupler for space radiation -induced SETs.

1) Application-Specific Testing: The transient response is very dependent on the application. For example, a larger load resistance increases the SET sensitivity [8], and the device is only sensitive when the coupler's LED is off (that is, when no light enters the photodetector). Therefore, the data must be collected for bias conditions that bound the application configuration (lower duty cycle, lower load).

2) Test Species and Energy Selection: In high-bandwidth optocouplers, both proton direct ionization and proton-induced nuclear reactions can cause SETs. Therefore, sensitivity should be investigated for a range of proton linear energy transfer (LET). This requires using a range of proton energies incident at both low and high angles of incidence [6]–[8]. Low-energy protons ($<$60 MeV) are needed to get the higher proton LET values, but they have a short range. (A 60-MeV proton has a range of about 18 mm in Si, while a 30-MeV proton has a range of just 5 mm in Si.) Therefore, the side of the package has to be ground away in order to allow low-energy protons to strike at large angles. If this is not done, scattering from the package will affect the results, producing protons with a distribution of lower energies.

The way the beam energy is obtained could also affect the results. The data in Fig. 3 show that a 60-MeV proton beam degraded to 30 MeV gives different results than a proton beam tuned to 30 MeV. The degraded beam gives higher cross sections, and the increase in cross section appears at lower angles. The increased width in the response around grazing incidence is due in part to the increase in beam divergence from multiple scattering interactions. Fig. 4 shows the results of TRIM calculations, indicating the change in proton trajectories resulting from degradation from 60- to 30-MeV average energy. In that case, again the scattering and energy straggling in the degrader material produce a distribution of protons with lower energies and, consequently, higher LETs.

Transients induced by heavy ions in the optocoupler's output amplifier can contribute to the total SET cross section and can last longer [9]. Heavy-ion testing should be considered if the single-event effect (SEE) environment is not dominated by protons, or if the coupler bandwidth is low and protons do not lead to SETs.

3) Proton Rate Prediction Method: Any proton-induced transient rate prediction technique for optocouplers must include effects due to direct and indirect ionization. Two

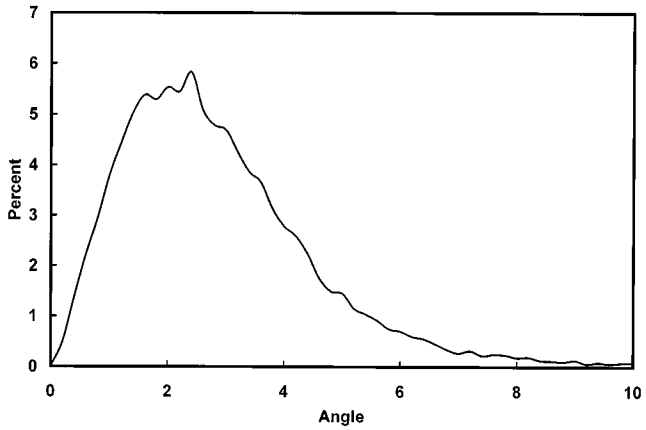

Fig. 4. TRIM calculation for trajectory of a 63-MeV proton after passing through 1.2 cm of Al. The exiting energy was ~30 MeV.

TABLE I
COMPARISON OF THE TRANSIENT RATES OBTAINED WITH THE TWO METHODS ON THE AGILENT 6N134 OPTOCOUPLER FOR A 705-km 98° CIRCULAR ORBIT BEHIND 100 mil OF Al SHIELDING, 50-mm THICKNESS

	Total number of transient/year	Number of transients/year induced by indirect ionization
Johnston method results (from [8]	1,665	470
Bendel-IRPP method results	1,200	400

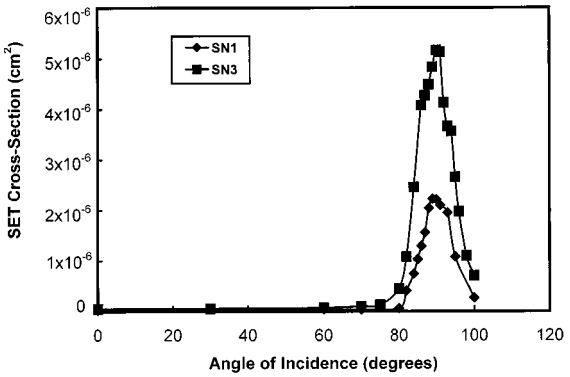

Fig. 5. Example of part-to-part dispersion observed during proton SET characterization of the Agilent HCPL5231.

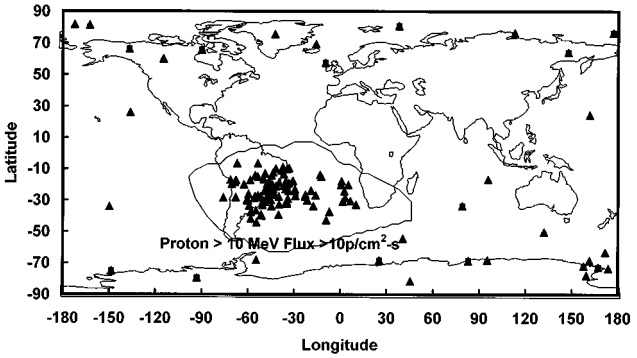

Fig. 6. Location of the Terra HGA events. These events have been shown to be a result of SETs induced in an Agilent HCPL5231.

approaches to SET rate predictions have been reported. Reed *et al.* recommended a combination of the Bendel method for proton-induced SET by nuclear reactions along with the traditional integral right rectangular parallelepiped (IRPP) method for direct ionization. It calls for using a LET distribution describing the combined proton and heavy-ion environments. Also, the cross section versus LET curve includes the combined proton and heavy-ion characterization results [7]. This approach is similar to the method recommended by Marshall and LaBel for the estimation of on-orbit performance of fiber-optic data links (FOLs) [10]. The geometry considered is an IRPP geometry. Unlike the pin diode structure commonly found in FOL receivers, the optocoupler's detectors use a conventional bipolar processing method; thus diffusion from the substrate bulk may be significant. Characteristics of optocoupler cross section measurement consistent with charge collection via diffusion were first noted in [6], and later investigations [8], [9] indicated that diffusions lengths approached 50 μm. For these thick aspect ratios, the ability of the RPP geometry to represent the actual circular cylindrical detector geometry could be a concern. This particular point is addressed in [11]. Johnston *et al.* recommended an empirical approach based on angular dependent SET cross section data measured at multiple proton energies [8]. Both methods give similar results, as shown in Table I. The advantage of the Bendel–IRPP method is that it uses the traditional tools for SEE rate prediction.

4) Device-to-Device Variability: Test data collected have shown significant part-to-part variability in optocoupler SET susceptibility. In Fig. 5, we can see a ratio greater than two between the maximum cross section for the two tested parts. (A 31-MeV proton beam energy was achieved by degrading a 63-MeV beam.) It is recommended that the test be performed on a sufficient number of parts coming from the flight lot.

C. Comparison of Bendel–IRPP Rate Prediction to On-Orbit Data

In this section, we present an example of an optocoupler that has experienced SETs in the space environment. The motor drive amplifier (MDA) of the high gain antenna (HGA) on the Terra satellite has experienced several anomalies (shutdown of the MDA) since the launch in December 1999. Analyses have shown that these anomalies are due to SETs in the Agilent HCPL-5231 optocouplers. Detailed studies of the flight hardware configuration showed that an SET-induced pulse lasting at least 100 ns on the output of the optocoupler could trigger this event.

Between December 20, 1999, and January 26, 2001, 135 anomalies were observed. Fig. 6 shows their location. Of these, 105 anomalies occurred in the South Atlantic anomaly (SAA) proton region. Among the 30 events that did not occur within the SAA, 23 occurred during the July 14th and November 9th solar particle events. The other seven events occurred in the high-latitude regions of the orbit and are attributed to galactic cosmic rays (GCRs).

SET testing was performed at the University of California at Davis (UCD) with protons and at Brookhaven National Laboratory (BNL) with heavy ions. During testing, the bias conditions were identical to the application conditions. Figs. 2, 3, and 5 present some of the proton SET cross section versus angle of incidence data. The data in Fig. 7 present our measured SET cross

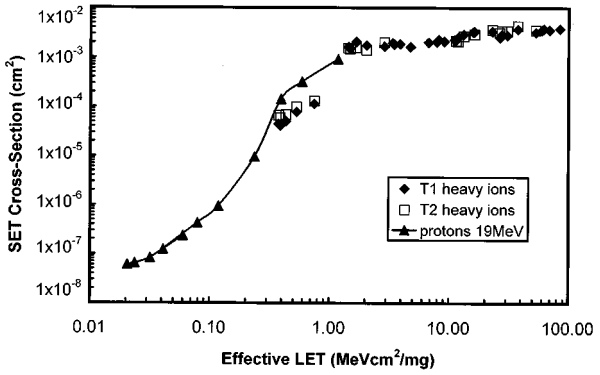

Fig. 7. Transient cross section for heavy-ion and proton effective LET.

section versus effective LET for heavy ions and protons. The proton cross section points are obtained by applying a $\cos(\theta)$ correction to the fluence used in the cross section calculation. Then we assign an effective LET, defined as the product of the particle's LET and $\sec(\theta)$. Note that the proton data and the low LET heavy-ion data are consistent. The LET dependence of both the heavy-ion and proton cross section data were then approximated by a Weibull distribution. The proton data at 0° incidence are used to build the proton cross section curve versus energy. This curve is then fitted with the Bendel model.

The CREME96 software was then used to define the environment (GCR and trapped protons integral LET spectra; and GCR protons and trapped protons energy spectra). The CREME96 HUP routine was used to calculate error contribution for direct ionization events, and the PUP routine was used to calculate the error rate for indirect ionization proton events. A discussion of the warnings and concerns when using CREME96 HUP for this type of calculation is given in [11].

The calculation was made assuming the solar maximum radiation environment for the Terra orbit (circular 690 km, 98° inclination orbit) and including the effects of 300-mil Al shielding. We also assumed a 50-mm sensitive volume depth to estimate the SET rates with PUP and HUP routines of CREME96. The estimated upset rate induced by GCRs is 0.05/d, and the upset rate induced by trapped protons is 1/d. Proton direct ionization accounted for about 70% of this rate. The total upset rate for the MDA is three times the upset rate of one optocoupler when the MDA motors are moving. These motors are moving about 40% of the time. So the estimated upset rate for the MDA is about 1.2/d. Since the observed rate is about one event every 3.3 d, this predicts the on-orbit rate to within a factor of four.

Based on the uncertainties in the prediction method (size of the sensitive volume, AP8 model uncertainties, absence of detailed shielding analyses, etc.) and the very significant part-to-part variation, we consider that the prediction is in very good agreement with the on-orbit event rate. The estimated upset rate for GCRs was ∼0.05/d, which is in good agreement with on-orbit data (∼20 predicted versus seven observed).

III. Assessment of Permanent Degradation

A. Introduction

Total ionizing dose (TID) and displacement damage Dose (DDD) can severely degrade the performance of an optocoupler. The most studied effect is how radiation degrades current transfer ratio (CTR). CTR is defined as the ratio of the output current (IC) to the input current (IF) (see Fig. 8). The concepts described here can be used to assess the degradation of any circuit parameter that depends on optocoupler CTR.

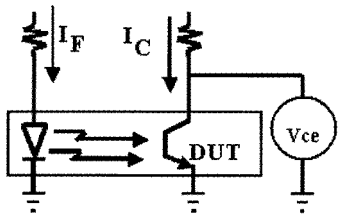

Fig. 8. Schematic showing experimental setup for measure CTR degradation.

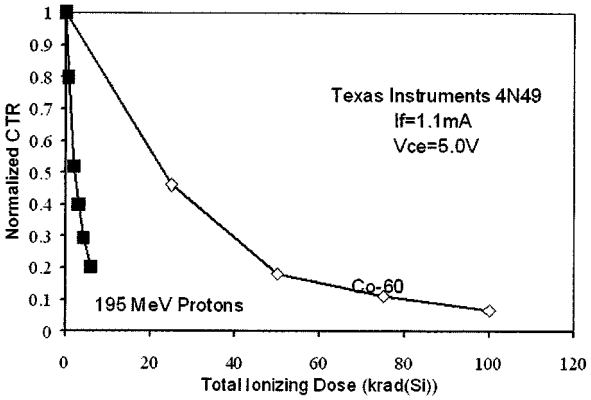

Fig. 9. Gamma and 195-MeV proton irradiations of Texas Instruments 4N49 [7].

Assessing radiation degradation of CTR is complicated by several factors.

1) Observed radiation-induced degradation results from a combination of ionizing dose and displacement damage mechanisms, each affecting the individual optocoupler components differently [1], [7].
2) Lack of consistency between experimental determination of damage factors for LEDs and theoretical calculations for nonionizing energy loss (NIEL) in III–V materials precludes use of NIEL to describe the energy dependence of displacement damage effects [12], [13].
3) Application-specific testing is necessary [5], [7].
4) Optocoupler radiation response exhibits large part-to-part variability.
5) Injection current can anneal the displacement damage-induced degradation of LED light output [4], [14].
6) Temperature and lifetime effects impact CTR [16].

Some of these concerns need to be addressed when estimating exposure levels, others during the testing phase of the risk assessment, and others must be considered in combination with radiation-induced degradation estimates to give overall performance. Each of these complications will be addressed in more detail during the discussion of the risk-assessment approach.

B. Risk-Assessment Approach

1) Introduction: TID and DDD can degrade the CTR of many optocouplers, as demonstrated in Fig. 9, which compares degradation for gamma-ray exposures of a Texas Instruments

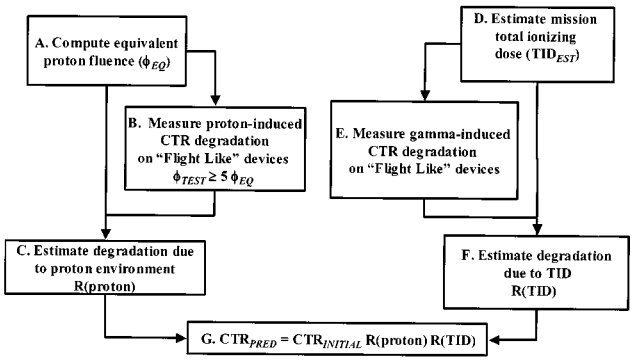

Fig. 10. Process for estimating CTR degradation.

(TI) 4N49 to that for 195-MeV proton exposures. Proton irradiations cause significantly larger degradation than gamma-ray exposures at equivalent doses. This type of optocoupler response is due to the greater amount of displacement damage for proton over gamma exposures [1]. A comprehensive radiation risk assessment must include both degradation mechanisms.

Fig. 10 shows our current approach for assessing the impact of the space radiation environment on optocoupler CTR. In this method, separate tests are conducted for both mechanisms. Then the results are combined to estimate the CTR degradation for a specific mission DDD and TID.

In this section of this paper, we will discuss each block of the radiation risk-assessment approach; the concerns listed above will be addressed when applicable.

2) Step A: Compute Equivalent Proton Fluence: It is beyond the scope of this paper to describe in detail how to compute the energy differential proton fluence for a mission. We refer the reader to [17] for a discussion on performing this calculation. This estimate should include any radiation design margins for environment variability.

A discussion of displacement damage effects on microelectronics and photonics is given in [15]. In this study, we utilize a combination of the methods defined in [15] for computing mission equivalent fluence from the predicted differential proton fluence to determine a worst case mission "equivalent" fluence ($\phi_{\rm EQ}$). The need to determine $\phi_{\rm EQ}$ is driven by the lack of consistency between theoretical calculations for NIEL in III–V materials and experimental determination of damage factors for LEDs (see [10, Figs. 8 and 9]).

The $\phi_{\rm EQ}$ is estimated by a "manufactured" worst case damage function. This function is constructed piecewise from segments of either the calculated NIEL curve for the specific III–V material [12] or the curve from experimental displacement damage measurements on the LEDs in question [9], [10]. The "manufactured" worst case curve is the combination of these curves that results in the worst case equivalent fluence for the test energy in question. The contributions to $\phi_{\rm EQ}$ from above and below the test energy are determined separately and added together to get $\phi_{\rm EQ}$. The $\phi_{\rm EQ}$ must be computed for each test energy.

3) Step B: Measure Proton-Induced Degradation: Proton testing is primarily used to assess the DDD effects on optocoupler CTR. However, for certain space flight missions that are dominated by a proton environment, proton testing can deliver sufficient TID to estimate both DDD- and TID-induced degradation. This will be discussed further in the section on TID effects.

The test fluence ($\phi_{\rm TEST}$) that should be used when performing ground testing to characterize optocoupler CTR degradation should be greater than a factor of five over $\phi_{\rm EQ}$. This is not a pass/fail fluence level; that is, it does not define the fluence level that should be used to simulate the expected on-orbit performance. Rather, it is a recommendation for the minimum value of the cumulative fluence used during the testing phase.

CTR must be measured prior to irradiation and at several fluence levels up to $\phi_{\rm TEST}$. Making multiple measurements of CTR allows for characterization of the degradation to be fully mapped out over $\phi_{\rm TEST}$ (for example, see proton data in Fig. 9). These data provide the CTR degradation curves used to estimate CTR degradation in Step C.

There are several test protocol issues that must be addressed when performing optocoupler CTR degradation measurements. Some of these were pointed out in the introduction to this section; we provide more detail on each issue here.

a) Proton test energies: Because of the inconsistency between experimental determination of damage factors for LEDs and theoretical calculations for NIEL [12], [13], we do not recommend using NIEL to determine the mission equivalent fluence for a single test energy. Instead, we recommend that a suite of energies be used. Proton test energy selection should be based on the expected space radiation environment (including shielding effects). An example of a suite of proton test energies for LEO mission with 100- mil shielding would be 200, 100, 60, 35 MeV, and lower if package penetration considerations allow knowledge of the energy reaching the internal components.

b) Application-specific testing: Device characterization must consider application specifics. For example, the response of the device depends on the drive current of the LED [1], [7] and the applied collector–emitter voltage for the photodetector [7]. In [7], we showed that fixing collector–emitter voltage (Vce) such that the photodetector is in the active region during testing can significantly overestimate the degradation of the device when the application calls for the device to operate in the saturation mode. Other application-specific issues should be considered carefully when preparing for a test.

c) Device-to-device variability: Since optocouplers are typically COTS hybrids, it is not surprising that they often exhibit large part-to-part variability. Some of this variation is due to the complication of having several different components that can be sensitive to various effects. Fig. 11 shows data collected on three Mitel 3C91C optocouplers. At certain fluences, there is over a factor of two variation in the response to radiation. This optocoupler is manufactured as a radiation-hardened product, and the internal components were all selected from the same device lot. These hybrids do not contain a light pipe to guide the light between the LED and the detector, so the variation is due to the differences in the response at the component level.

Another reason for part-to-part variations (and the most difficult to characterize) is the flexibility the vendor has in selecting the components internal to the optocoupler. Fig. 12 gives data on

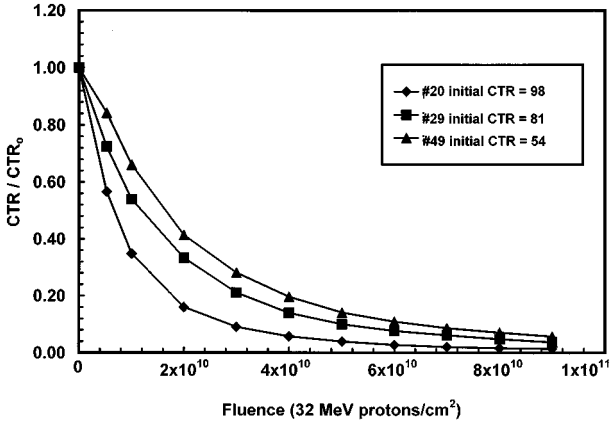

Fig. 11. Demonstration of part-to-part variability of CTR degadation within a single lot.

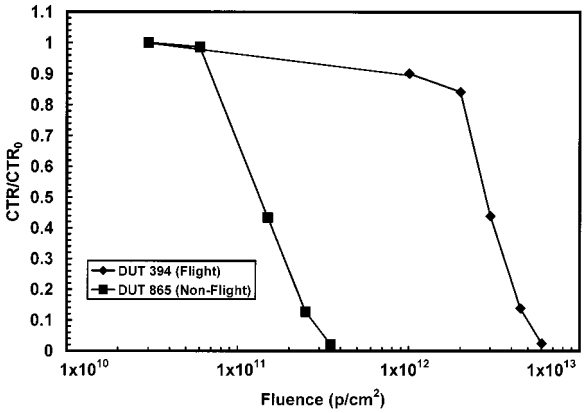

Fig. 12. Demonstration of lot-to-lot variability of CTR degradation.

Mirocpac 4N49. These data show as much as an order of magnitude variation in the sensitivity of these optocouplers from different "lots." As with all COTS devices, knowledge of the manufacturing process is very limited. Our recommendation is to acquire optocouplers from vendors with a history of providing devices that have consistent degradation characteristics, to test the devices from the "flight-like" lot in a "flight-like" configuration, and realize that there is still some unquantified inherent risk. This risk is inherent in the choice to use COTS on a space flight mission—a risk that must be accepted at the beginning of the mission design.

d) Annealing of damage: Injection current annealing of displacement damage-induced degradation of LED light output has been observed [4], [14]. This has also been observed in optocouplers. Fig. 13 shows the recovery of the collector current under two annealing currents (1 and 10 mA) for three measurement forward currents (1, 5, and 10 mA). The data connected with the solid lines were annealed at 10 mA (unfilled symbols), while the data represented by the filled symbols were taken at 1-mA annealing forward current. The collector current is normalized to the preirradiation values. The ordinate is the amount of charge in coulombs that has passed through the LED during the annealing period. (So for 10-mA anneal, the time to reach 1800 C is 50 h, while the time to reach this charge for a 1-mA anneal is 20.8 d.) The recovery factor shown in the legend gives the ratio of the collector current after 1800 C anneal to postirradiation (prior to the anneal step) values for the collector current.

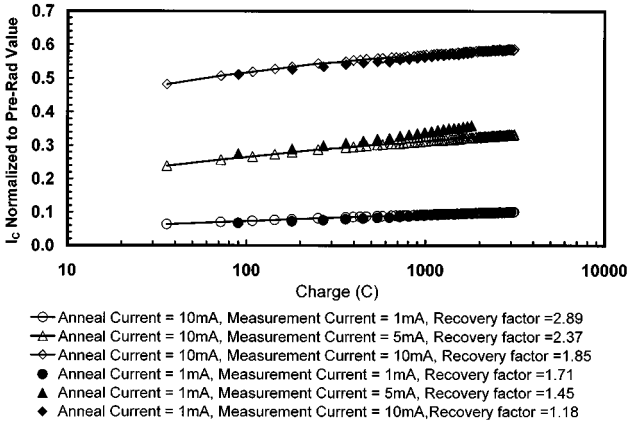

Fig. 13. Injection current annealing effect on collector current at two forward currents for three application currents. The data are normalized to the preirradiation collector currents.

First note that for the annealing conditions between 100 and 1800 C, there is a correlation of the recovery between the 1- and 10-mA annealing conditions for all three test conditions. This implies that an accelerated annealing test could be used for these annealing periods, reducing the time to determine the amount of recovery by a factor of ten. If this accelerated annealing approach could be generalized, then one could use it to estimate the annealing occurring over long mission times. However, in order to generalize this accelerated annealing test, more data on other part types are needed. Also, for missions with long annealing times, studies out to greater integral charge values will be required. This accelerated annealing approach should be studied in more detail before being implemented in a risk-assessment approach.

The second interesting point that these data show is that the collector-current recovery factor (the ratio of the annealed collector current to the postirradiation value) is dependent on the forward current and the annealing current. The recovery factor is also dependent on the anneal time. All of these are application-dependent issues.

Annealing should be minimized while collecting CTR degradation data over the test fluence. This can be best achieved if the optocoupler "on-time" (when the LED is illuminating the photodetector) is minimized and the forward current is minimized. Postirradiation annealing studies at the anticipated forward current conditions and the "on-time" for the on-orbit application can be used to understand the margin in the final estimate of the on-orbit degradation (Step G).

4) Step C: Estimation of Proton-Induced Degradation: Testing over a range of energies allows the degradation to be estimated using a piecewise approach. The method bins the predicted (including any design margin requirements) space radiation particle fluence by test energy, and then uses the experimental CTR degradation curves (like those in Figs. 9, 11, and 12) to determine the total degradation. For example, using the test energy suite for a given environment, one would sum up all particles with energies between 100 and 200 MeV and use the higher of the two measured CTR degradation rates over this energy range to estimate the degradation for this energy range. One would repeat this procedure for all energy ranges. The net degradation would be the sum over all energy bins.

For protons with energies too low to penetrate the package during ground testing, one must use the energy dependence of the calculated NIEL to estimate the damage rate. We strongly recommend that this only be used for energies less than 30 MeV, a region where the functional dependence of the calculations for NIEL nearly agrees with that for experimental data obtained on LEDs [9], [10].

The sum of the estimated damage computed for each energy bin plus any additional degradation from lower energy protons gives an estimate of proton-induced on-orbit CTR degradation. R(proton) is defined as the ratio of the proton-induced degraded CTR to the initial CTR.

This test and analysis approach also lends itself to assessment of shielding alternatives since the impact of reducing the lower energy protons is readily apparent.

We now move to the TID side of Fig. 10.

5) Step D: Estimate Mission Total Ionizing Dose: It is beyond the scope of this paper to describe in detail the methods used to compute the estimated mission TID ($\mathrm{TID_{EST}}$). We refer the reader to [17] for a discussion on performing this calculation. This estimate should include any radiation design margins for environment variability.

6) Step E: Measure Gamma-Induced CTR Degradation: The discussion given in Step B recommended using protons as the test environment for DDD effects. As discussed above, protons can also contribute significantly TID-induced degradation. We contend that if the mission TID level can be achieved during proton DDD testing, then the DDD- and TID-induced degradation of CTR is sufficiently measured during the proton testing, and TID testing using another ionizing dose source need not be carried out. However, if the TID delivered by the proton testing in Step B is less than that delivered by the on-orbit ionizing dose sources, then both proton testing (for DDD effects) and gamma (or any other ionizing dose source that has very limited DDD effects) testing must be carried out. The discussion that follows addresses "gamma-style" TID testing. Typically, gamma- or X-ray testing is used to simulate the space radiation TID environment. The dose level for TID testing ($\mathrm{TID_{TEST}}$) should follow the guidelines in ASTM Standard 883: Test Method 1019.5. TID testing should include attention to application-specific details (see discussion in Step B).

CTR must be measured prior to irradiation and at several TID steps up to $\mathrm{TID_{TEST}}$; for example, see Co-60 data in Fig. 9. These data provide the CTR degradation curves used to estimate CTR degradation in Step F.

7) Step F: Estimation of TID-Induced Degradation: The degraded CTR is determined by the estimated mission TID (Step D) and the measured CTR degradation (Step E). The estimates should follow the guidelines in ASTM Standard 883: Test Method 1019.5. R(proton) is defined as the ratio of the degraded CTR value to the initial CTR.

8) Step G: Estimation of Degradation: Multiplying the TID- and proton-induced degradations gives an estimate for the on-orbit CTR degradation ($\mathrm{CTR_{PRED}}$)

$$\mathrm{CTR_{PRED}} = \mathrm{CTR_{INITIAL}}\mathrm{R(TID)R(proton)} \qquad (1)$$

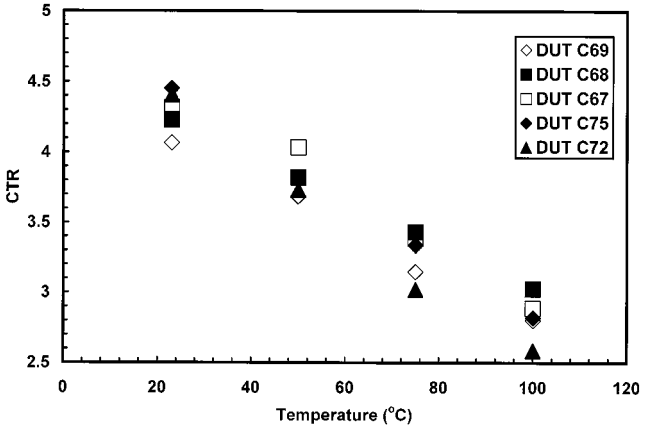

Fig. 14. Temperature effects on CTR for an Isolink 4N49 optocoupler.

where $\mathrm{CTR_{INITIAL}}$ is the initial CTR. This will allow one to determine the CTR margin that exists in a specific application. The margin is the ratio of the minimum CTR required to keep the application functional to $\mathrm{CTR_{PRED}}$.

C. Recommendations and Final Comments

The approach defined above will yield a conservative estimate for CTR degradation. This is in part due to the exclusion of any annealing that may occur, in part that protons can induce damage via TID and displacement damage, and finally in part to the use of a worst case "equivalent" fluence estimate. Although the above approach can be modified to account for these effects (albeit with reduced margins), we prefer to retain a conservative estimate—especially given the uncertainties associated with the use of COTS hybrid devices.

Temperature effects must also be considered when using the margins derived above to assess the likelihood of optocoupler survival when exposed to the space radiation environment. The data in Fig. 14 show that for an Isolink 4N49, there is a 30–40% decrease in the CTR when the device is warmed from room temperature ($\sim$23 °C) to 100 °C. Flight temperature conditions must be considered when assessing the performance of an optocoupler in a space flight application.

Also, optocoupler reliability issues like LED aging effects must be considered when assessing on-orbit performance. In [16], it was shown that aging effects do not impact radiation-induced degradation characterization. However, the end-of-mission aging effects on LED must be considered when assessing optocoupler survivability.

Finally, we would like to remind the reader that double heterojunction LEDs typically show less degradation than either amphoterically doped or single heterojunction LEDs. When such a selection is possible, a device that uses a double heterojunction LED will survive longer in the space radiation environment.

IV. Conclusions

The challenges of risk assessment for parametric degradation and single-event transients in optocouplers for satellite applications are compounded by the COTS/hybrid nature of these

devices. We have discussed approaches that have been developed for estimating this risk, although the development of a rigorous RHA program for optocouplers remains a task for the future. In developing these techniques, we have benchmarked our estimates for proton and heavy-ion induced SET rates with recent flight data from the Terra mission and found good agreement. For CTR degradation, we have outlined a semi-empirical method for acquiring test data and using these data in conjunction with the important factors affecting device CTR to estimate CTR radiation response. The method considers the circuit application, environment, damage energy dependence, device response to TID and displacement effects, temperature, and annealing. Although the approach is probably conservative, we would argue that given the number and nature of the variables that the approach addresses, a conservative approach is warranted. We have adopted these methods to aid in risk management for NASA missions.

ACKNOWLEDGMENT

The authors would like to thank R. Ladbury for insightful technical discussion and review of this paper. They would also like to thank D. Cochran and M. O'Bryan for support while preparing this manuscript.

REFERENCES

[1] G. Rax, C. I. Lee, and A. H. Johnston, "Total dose and proton damage in optocouplers," *IEEE Trans. Nucl. Sci.*, vol. 43, pp. 3167–3173, Dec. 1996.

[2] A. S. Epstein and P. A. Trimmer, "Radiation damage and annealing effects in photon coupled isolators," *IEEE Trans. Nucl. Sci.*, vol. NS-19, pp. 391–399, Dec. 1972.

[3] K. J. Soda, C. E. Barnes, and R. A. Kiehl, "The effect of gamma irradiation on optical isolators," *IEEE Trans. Nucl. Sci.*, vol. NS-22, pp. 2475–2481, Dec. 1975.

[4] C. E. Barnes and J. J. Wiczer, "Radiation effects in optoelectronic devices," Sandia, Rep. SAND84-0771, 1984.

[5] M. D'Ordine, "Proton displacement damage in optocouplers," in *IEEE Radiation Effects Data Workshop*, July 1997, pp. 122–124.

[6] K. A. LaBel, P. W. Marshall, C. J. Marshall, M. D'Ordine, M. A. Carts, G. Lum, H. S. Kim, C. M. Seidleck, T. Powell, R. Abbott, J. L. Barth, and E. G. Stassinopoulos, "Proton-induced transients in optocouplers: In-flight anomalies, ground irradiation test, mitigation and implications," *IEEE Trans. Nucl. Sci.*, vol. 44, pp. 1885–1892, Dec. 1997.

[7] R. A. Reed, P. W. Marshall, A. H. Johnston, J. L. Barth, C. J. Marshall, K. A. LaBel, M. D'Ordine, H. S. Kim, and M. A. Carts, "Emerging optocoupler issues with energetic particle-induced transients and permanent radiation degradation," *IEEE Trans. Nucl. Sci.*, vol. 45, pp. 2833–2841, Dec. 1998.

[8] A. H. Johnston, T. Miyahara, G. M. Swift, S. M. Guertin, and L. D. Edmonds, "Angular and energy dependence of proton upset in optocouplers," *IEEE Trans. Nucl. Sci.*, vol. 46, pp. 1335–1341, Dec. 1999.

[9] A. L. Barry, A. J. Houdayer, P. F. Hinrichsen, W. G. Letourneau, and J. Vincent, "The energy dependence of lifetime damage constants in GaAs LED's for 1–500MeV protons," *IEEE Trans. Nucl. Sci.*, vol. 42, pp. 2104–2107, Dec. 1995.

[10] R. A. Reed, P. W. Marshall, C. J. Marshall, R. L. Ladbury, H. S. Kim, L. X. Nguyen, J. L. Barth, and K. A. LaBel, "Energy dependence of proton damage in AlGaAs light emitting diodes," *IEEE Trans. Nucl. Sci.*, vol. 47, pp. 2492–2499, Dec. 2000.

[11] A. H. Johnston, B. G. Rax, L. E. Selva, and C . E. Barnes, "Proton degradation of light-emitting diodes," *IEEE Trans. Nucl. Sci.*, vol. 46, pp. 1781–1789, Dec. 1999.

[12] P. W. Marshall and C. J. Marshall, "Proton effects and test issues for satellite applications," in *Proc. IEEE NSREC99 Short Course*, July 1999.

[13] A. H. Johnston and T. F. Miyahara, "Characterization of proton damage in light emitting diodes," *IEEE Trans. Nucl. Sci.*, vol. 47, pp. 2500–2507, Dec. 2000.

[14] A. H. Johnston, G. M. Swift, T. Miyahara, S. M. Guertin, and L. D. Edmonds, "Single-event upset effects in optocouplers," *IEEE Trans. Nucl. Sci.*, vol. 45, pp. 2867–2875, Dec. 1998.

[15] P. W. Marshall, C. J. Dale, and K. A. LaBel, "Space radiation effects in high performance fiber optic data links for satellite data management," *IEEE Trans. Nucl. Sci.*, vol. 43, pp. 645–653, Apr. 1996.

[16] P. W. Marshall, "Test needs and error rate predictions approaches for single event transients in fiber optic link detectors and optocouplers," presented at the RADECS 2001.

[17] J. L. Barth, "Modeling space radiation environments," in *IEEE NSREC99 Short Course*, July 1999.

[18] K. A. LaBel, S. D. Kniffin, R. A. Reed, H. S. Kim, J. L. Wert, D. L. Oberg, E. Normand, A. H. Johnston, G. K. Lum, R. Koga, S. Crain, J. R. Schwank, G. L. Hash, S. Buchner, J. Mann, L. Simpkins, M. D'Ordine, C. J. Marshall, M. V. O'Bryan, C. M. Seidleck, L. X. Nguyen, M. A. Carts, R. L. Ladbury, and J. W. Howard, "A compendium of recent optocoupler radiation test data," in *IEEE Radiation Effects Data Workshop*, July 2000, pp. 123–146.